Determining the fraction of compact objects in the Universe using supernova observations

E. Mörtsell*, A. Goobar†, and L. Bergström‡
Department of Physics, Stockholm University,
Box 6730, S–113 85 Stockholm, Sweden

We investigate the possibility to determine the fraction of compact objects in the Universe by studying gravitational lensing effects on Type Ia supernova observations. Using simulated data sets from one year of operation of the proposed dedicated supernova detection satellite SNAP, we find that it should be possible to determine the fraction of compact objects to an accuracy of $\lesssim 5\%$.

I. INTRODUCTION

Recent measurements of anisotropies in the cosmic microwave background radiation (CMBR) show that the Universe is very close to flat, i.e., $\Omega_{\rm tot} \approx 1$ [1,2]. Since observations of Type Ia supernovae (SNe) indicate that the expansion rate of the Universe is accelerating, the major part of this total energy should have negative pressure, e.g., in the form of the cosmological constant corresponding to $\Omega_\Lambda \sim 0.7$ in a flat universe [3,4], in agreement with constraints on the matter density $\Omega_{\rm M}$ from cluster abundances [5,6] and large-scale structure [7]. Thus, a a concordance model with $\Omega_{\rm M} \approx 0.3$ and $\Omega_\Lambda \approx 0.7$ has emerged.

The constitution of the total matter density is a matter of intense theoretical and experimental research. The energy density in baryonic matter as derived from Big Bang nucleosynthesis (BBN) is given by $\Omega_{\rm b}h^2 = 0.019 \pm 0.0024$ [8] whereas CMBR measurements yield a somewhat higher value; $0.022 < \Omega_{\rm b}h^2 < 0.040$ [9]. Either way, the matter density in baryons is almost one order of magnitude smaller than the non-baryonic dark matter (DM) component. However, the BBN range for the baryon density still means that most of the baryonic matter is also dark.

There are various possibilities for the dark baryons to hide, examples are warm gas in groups and clusters (which is difficult to detect at present [10]), or in the form of massive compact halo objects (MACHOs), where indeed there have been detections [11,12]. The long lines of sight to distant supernovae means that they are well suited to probe the matter content along the paths of the light rays, where gravitational lensing may occur where there are matter accumulations. Compact objects give more distinct lensing effects, enabling a distinction between diffuse matter and compact bodies along the light path. In particular, it may be possible to investigate whether the halo fraction deduced for the Milky Way from microlensing along the line of sight to the Large Magellanic Cloud, of the order of 20 % [11], is a universal number or if the average cosmological fraction is larger or smaller.

Regardless of its constitution, we can classify dark matter according to its clustering properties. In this paper we will use the terminology of *smooth DM* for DM candidates which tend to be smooth on subgalaxy scales, e.g., weakly interacting massive particles (WIMPs) such as neutralinos. The term *compact DM* will be reserved for MACHOs such as brown or white dwarfs and primordial black holes (PBHs) [13].

An advantage with gravitational lensing is that its effects can determine the distribution of dark matter independent of its constitution or its dynamical state. The topic of this paper concerns the use of the gravitational magnification of standard candles, such as Type Ia SNe, to determine the fraction of compact objects in a cosmological context.

In an early study, Rauch [14] concluded that with a sample of 1000 Type Ia SNe at redshift $z \approx 1$, one should be able to discriminate between the extreme cases of all DM as smooth or in compact objects. More recent work (Metcalf and Silk [15], Goliath and Mörtsell [16]) has shown that a sample of 50–100 SNe should be sufficient to make the same discrimination. Seljak and Holz [17] have found that it should be possible to actually determine the fraction of compact objects to 20 % accuracy with 100–400 Type Ia SNe at $z = 1$. In this work we extend these studies by exploring the possibility to determine the fraction of compact objects using a future sample of Type Ia SNe distributed over a broad redshift range, with the intrinsic spread of absolute luminosity of the SNe and expected measurement error for a proposed space-borne mission, SNAP [18] taken into account.

In Sec. II we clarify the distinction between compact and non-compact dark matter objects. In Sec. III we discuss gravitational lensing of SNe and in Sec. IV, we present the Monte-Carlo simulation package used to predict this effect. Sec. V is concerned with the proposed satellite telescope which will be able to produce the data sets used in this study and in Sec. VI we present our results. The paper is concluded with a summary in Sec. VII.

*E-mail address: edvard@physto.se
†E-mail address: ariel@physto.se
‡E-mail address: lbe@physto.se

II. COMPACT OBJECTS

For an object to be compact in a lensing context, we demand that it is contained within its own Einstein radius, r_E. For a DM clump at $z = 0.5$ and a source at $z = 1$, $r_E \sim 10^{-2}(M/M_\odot)^{1/2}$ pc in a $\Omega_{\rm M} = 0.3, \Omega_\Lambda = 0.7$ and $h = 0.65$ cosmology. Also, the Einstein radius projected on the source plane should be larger than the size of the source. A Type Ia SN at maximum luminosity has a size of $\sim 10^{15}$ cm, implying a lower mass limit of $\sim 10^{-4} M_\odot$ for the case described above.

The effects of lensing by compact objects are different from those of lensing by halos consisting of smoothly distributed dark matter, such as in the singular isothermal sphere or Navarro-Frenk-White density profile (NFW; [19]), the main difference being the tail of large magnifications caused by small impact-parameter lines of sight near the compact objects. However, N-body simulations predict, besides the overall cuspy profiles of ordinary Galaxy-sized dark matter halos, also a large number of small subhalos on all length scales which can been resolved [19,20]. The number density of the smaller objects, of mass M, follows approximately the law $dN/dM \propto M^{-2}$ as predicted by Press-Schechter theory. Thus one may expect a multitude of subhalos in each galaxy or cluster halo. In addition, N-body simulations show the less massive halos to be denser (mainly due to them being formed early when the background density was higher). Thus, it is appropriate to address the question whether this type of small-scale structure, and in particular the dense central regions of them, may give rise to lensing effects similar to the ones caused by truly compact objects.

To put a bound of these possible effects, we use the results of the most accurate numerical simulations to date [20]. The density profiles within dark matter clumps obtained in the simulations can be fit by the Moore profile

$$\rho_M(r) = \frac{\rho'_M}{\left(\frac{r}{a}\right)^{1.5}\left(1+\left(\frac{r}{a}\right)^{1.5}\right)} \tag{1}$$

Here ρ'_M and a are not independent parameters, but related by the concentration parameter $c_M = R_{200}/a$, which depends on mass roughly as

$$c_M \sim 10.6 M_{12}^{-0.084}. \tag{2}$$

(Here M_{12} is the virial mass in units of 10^{12} $M_\odot$; R_{200} is the virial radius where the average overdensity is 200 times the background density. Similar relations appear in the NFW simulations.)

Using these relations we can derive the mass M_R (also in units of 10^{12} $M_\odot$) within distance R_{pc} parsecs from the center of the halo,

$$M_R \sim 10^{-7} M_{12}^{0.4} R_{pc}^{1.5} \tag{3}$$

Comparing this with the Einstein radius for the same mass for a lensing event of typical distance D_{Gpc} Gigaparsecs,

$$R_E \sim 10^4 M_R^{0.5} D_{Gpc}^{0.5} \text{ pc}, \tag{4}$$

we find that M_R is within its own Einstein radius if

$$M_R \lesssim 10^{-4} M_{12}^{1.6} D_{Gpc}^3. \tag{5}$$

The requirement that the lensing mass is greater than $10^{-4} M_\odot$ means that dark matter clumps of the Moore type with mass greater than around $10^4 M_\odot$ ($M_{12} > 10^{-8}$) will in principle contribute to compact lensing. However, it is only the very central, dense core that can contribute to the lensing, and we see from Eq. (5) that only a small fraction f of the mass in the clump is within its own Einstein radius,

$$f = \frac{M_R}{M_{12}} \sim 10^{-4} M_{12}^{0.6} D_{Gpc}^3. \tag{6}$$

Thus only clumps of Galaxy size contribute appreciably to the lensing, and this part is included in our standard calculations.

Since this analysis was made for Moore-type halos, which are more concentrated than NFW halos, we conclude that compact objects detected through lensing of supernovae cannot, according to current thinking about structure formation, be caused by clumps of particle dark matter formed through hierarchical clustering.

III. GRAVITATIONAL LENSING OF SUPERNOVAE

The effect of gravitational lensing on Type Ia SN measurements is to cause a dispersion in the Hubble diagram. In Fig. 1 we compare the dispersion due to gravitational lensing with the intrinsic dispersion and the typical measurement error for Type Ia SNe. In the upper left panel, we show an ideal Hubble diagram with no dispersion and in the upper right panel we have added the dispersion due to lensing (lens) in a universe with 20 % compact objects and 80 % smooth dark matter halos parametrized by the Navarro-Frenk-White formula [19]. Comparing with the panel in the lower left where the intrinsic dispersion (intr) and measurement error (err) have been included, we see that the effects become comparable at a redshift of unity. In the lower right we see the most realistic simulation with intrinsic dispersion, measurement error and lensing dispersion.

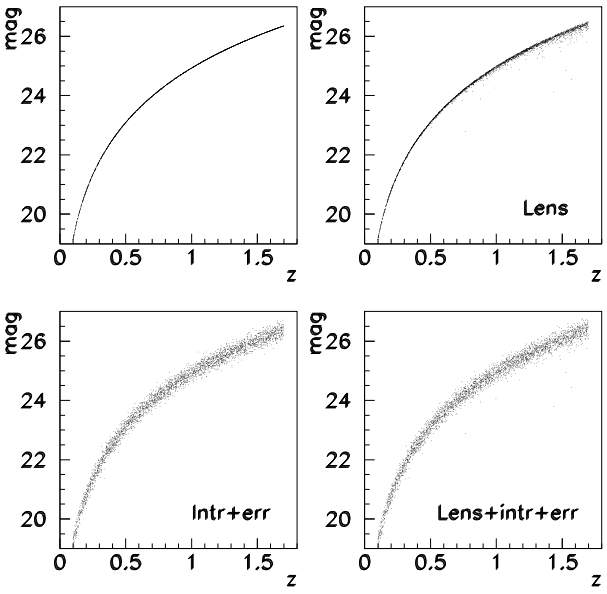

FIG. 1. A comparison of the dispersion due to lensing (upper right) and the measurement error and intrinsic dispersion of Type Ia SNe (lower left).

Of course, the additional dispersion caused by gravitational lensing will be a source of systematic error in the cosmological parameter determination with Type Ia supernovae. However, a possible virtue of lensing is that the distribution of luminosities might be used to obtain some information on the matter distribution in the Universe, e.g., to determine the fraction of compact DM in our Universe.

IV. SUPERNOVA OBSERVATION CALCULATOR

To perform realistic calculations we have developed a numerical simulation package, SNOC (the SuperNova Observation Calculator). It can be used to estimate various systematic effects such as dust extinction and gravitational lensing on current SN measurements as well as the accuracy to which various parameters can be measured with future SN searches. In this paper, we use SNOC to obtain simulated samples of the intrinsic dispersion and gravitational lensing effects of Type Ia SNe over a broad redshift range.

The intrinsic dispersion and measurement error is represented by a Gaussian distribution with $\sigma_m = 0.16$ mag. Gravitational lensing effects are calculated by tracing the light between the source and the observer by sending it through a series of spherical cells in which the dark matter distribution can be specified. For more details on the method, originally proposed by Holz and Wald, see [21,22].

We will model compact DM as point-masses and smooth DM as the Navarro-Frenk-White density profile. The exact parameterization of the smooth DM halo profile is not important for the results obtained in this paper [22]. The results are also independent of the individual masses of the compact objects as well as their large scale clustering properties [21,22]. As we have seen, the eventual small-scale structure in the "smooth" component does not act as a compact component.

V. SUPERNOVA/ACCELERATION PROBE

To make realistic predictions of the statistics and quality of the supernova sample, we use the projected discovery potential of the Supernova/Acceleration Probe (SNAP) project. This is a proposed satellite telescope capable of discovering over 2000 Type Ia SNe per year in the redshift range $0.1 < z < 1.7$ [18]. The most anticipated use of the data is to gain further accuracy in the determination of, e.g., $\Omega_{\rm M}$ and the curvature of the Universe $\Omega_{\rm k}$, but also to give insight into the nature of the negative pressure energy component by constraining the equation of state [23,24], or the redshift dependence of the effective energy density [25]. Here we show how the data also can be used to give information on the fraction of compact objects in the dark matter component.

More specifically, it is projected that in one year, SNAP will be able to discover, follow the light curves and obtain spectra for of the order of 2000 SNe. While the exact redshift distribution of the Type Ia supernovae to be followed by SNAP might be changed upon studies of the optimal search strategies for the primary goals of the project, we have used the Monte-Carlo generated sample spectra of 2366 SNe distributed according to the SNAP proposal [18], see Fig. 2, to make specific predictions.

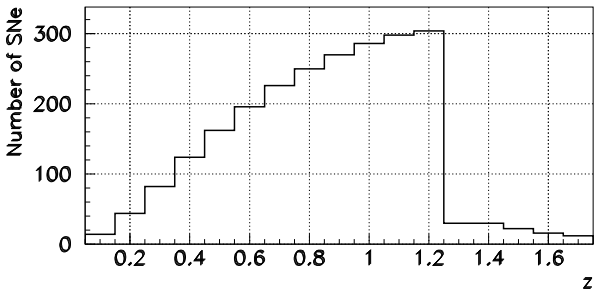

FIG. 2. Number of Type Ia SNe expected for various redshift bins in a one-year exposure with the proposed SNAP satellite. The data are taken from Table 7.2 in the SNAP science proposal [18].

VI. RESULTS

Using SNOC, we have created large data sets of synthetic SNe observations with a variable fraction of com-

pact objects ranging from 0 to 40 % using the following cosmological background parameter values: $\Omega_{\rm M} = 0.3, \Omega_\Lambda = 0.7$ and $h = 0.65$. (For a discussion of how the halo distributions were generated, see [22].) These are used as reference samples. In Fig. 3, we have plotted the dispersion in the reference samples for 0 % (full line), 20 % (dashed line) and 40 % (dotted line) compact objects. In the upper panel, the lensing dispersion is plotted, i.e., the dashed line basically corresponds to the scatter in the upper right panel in Fig. 1. The zero value corresponds to the value one would obtain in a homogeneous universe (upper left panel in Fig. 1). Note that negative values correspond to magnified events, positive values to demagnified events. It is clear, that as the fraction of compact DM grows, lensing effects becomes larger in the sense that we have a larger fraction of highly magnified events. In the lower panel we have added a Gaussian intrinsic dispersion and measurement error, $\sigma_{\rm m} = 0.16$ mag, making the distributions look more similar (cf., lower right panel in Fig. 1). Although this smearing obviously decreases the significance of the compact signal, it can be seen that the high-magnification tails still are clearly visible.

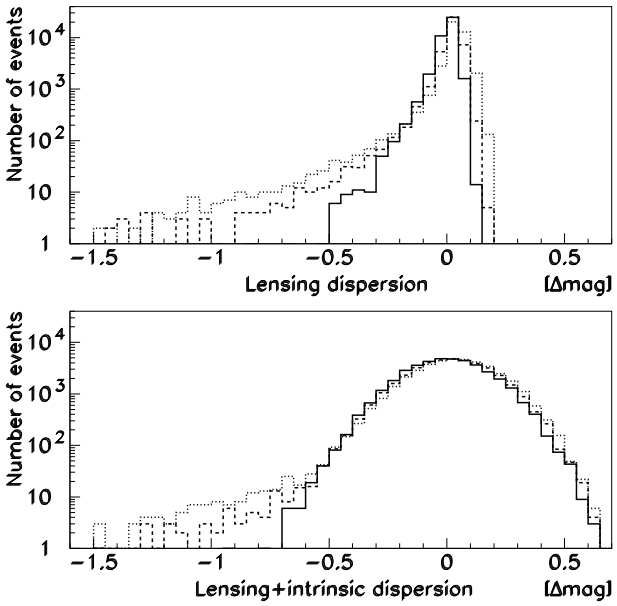

FIG. 3. Magnitude dispersion of reference samples for 0 % (full line), 20 % (dashed line) and 40 % (dotted line) compact objects. The bottom panel includes a Gaussian smearing, $\sigma_{\rm m} = 0.16$ mag, due to intrinsic brightness differences between supernovae and from measurement error. The distributions show the projected scatter around the ideal Hubble diagram for Type Ia supernovae with a relative redshift distribution as in Fig. 2.

We have also created a large number of simulated one-year SNAP data sets (according to Fig. 2 above) with 6, 11 and 21 % compact objects. These are our experimental samples. By comparing each generated experimental sample with our high-statistics reference samples using the Kolmogorov-Smirnov (KS) test, we obtain a confidence level for the hypothesis that the experimental sample is drawn from the same distribution as the reference sample. For each fraction of compact objects in the experiments (6, 11 and 21 %), we repeat this procedure for 1000 experimental realizations and pick out the reference sample which gives the highest confidence level for each experiment. Plotting the number of best-fit reference samples as a function of the fraction of compact objects in the reference sample, we can fit a Gaussian and thus estimate the true value and the dispersion. In each case, we get a mean value within 1 % of the true value and a one-sigma error less than 5 %, see Fig. 4.

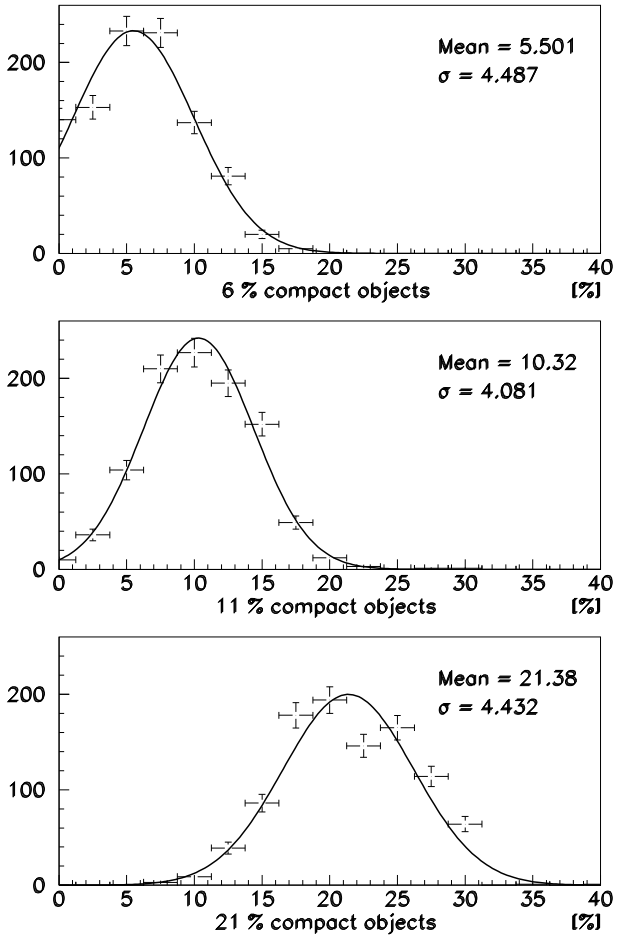

FIG. 4. The number of best-fit reference samples as a function of the fraction of compact objects in the reference sample.

As one could expect, and is shown in Fig. 1, lensing effects get larger at higher redshifts. At low redshifts the dispersion is completely dominated by the intrinsic dispersion. Therefore, we have only used the data from SNe at $z > 0.8$, a total of 1387 SNe, to obtain the result

in Fig. 4.[1]

In this analysis, we have assumed that $\Omega_{\rm M}$ and Ω_Λ will be known to an accuracy where the error in luminosity is negligible in comparison to the intrinsic and lensing dispersion of Type Ia SNe. This assumption is not unreasonable with future CMBR observations combined with other cosmological tests and the SNAP data itself, nor is it crucial in the sense that we are dealing with the dispersion of luminosities around the true mean value, not the mean value itself. In order to test the sensitivity of our results to changes in the cosmological parameter values, we have performed a number of Monte-Carlo simulations using different sets of parameters in our experimental and reference samples and found the error in the total energy density in compact objects to be negligible[2]. Also, we have used a value of the intrinsic dispersion and measurement error of $\sigma_{\rm m} = 0.16$ mag, a value which may be appreciably smaller in the future when the large data sample expected may allow, e.g., a more refined description and classification of supernovae. Using simulated data sets with $\sigma_{\rm m} = 0.1$ mag, the one-sigma error in the determination of the fraction of compact objects, using the same cosmology as above, becomes less than 3 %, as depicted in Fig. 5.

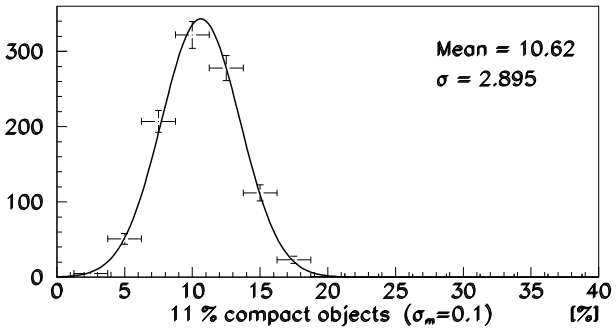

FIG. 5. The number of best-fit reference samples as a function of the fraction of compact objects in the reference sample for an intrinsic dispersion and measurement error of $\sigma_{\rm m} = 0.1$ mag.

[1]Of course, the data from SNe at $z < 0.8$ can still be used to constrain the values of $\Omega_{\rm M}$ and Ω_Λ. In fact, with one year of SNAP data, it is possible to determine $\Omega_{\rm M}$ with a statistical uncertainty of $\Delta\Omega_{\rm M} \approx 0.02$ [18].

[2]Note that the effect from lensing is proportional to the total energy density in compact objects, not the fraction of compact objects, see, e.g., [26]. A higher $\Omega_{\rm M}$ would therefore increase the sensitivity for smaller fractions.

VII. SUMMARY

The proposed SNAP satellite will be able to detect and obtain spectra for more than 2000 Typa Ia SNe per year. In this paper we have used simulated data sets obtained with the SNOC simulation package to show how one-year SNAP data can be used to determine the fraction of compact DM in our Universe to $\lesssim 5\%$ accuracy, assuming the intrinsic dispersion and measurement error is $\sigma_{\rm m} = 0.16$ mag. If the intrinsic dispersion and measurement error can be further reduced, e.g., from a improved understanding of Type Ia SN detonation mechanisms, the accuracy can be improved even further.

ACKNOWLEDGEMENTS

LB wishes to thank the Swedish Research Council for financial support, and the Institute for Advanced Study at Princeton for hospitality when part of this work was performed. AG is a Royal Swedish Academy Research Fellow supported by a grant from the Knut and Alice Wallenberg Foundation.

[1] P. de Bernardis *et al.*, Nature 404 (2000) 955.
[2] A. Balbi *et al.*, *pre-print* astro-ph/0005124 (2000).
[3] S. Perlmutter *et al.*, Astrophys. J. 517 (1999) 565.
[4] A.G. Riess *et al.*, Astronom. J. 116 (1998) 1009.
[5] N.A. Bahcall and X. Fan, Astrophys. J. 504 (1998) 1.
[6] R.G. Carlberg *et al.*, Astrophys. J. 516 (1998) 552.
[7] J.A. Peacock *et al.*, Nature, 410 (2001) 169.
[8] S. Burles *et al.*, Phys. Rev. Lett. 82 (1999) 4176.
[9] M. Tegmark and M. Zaldarriaga, Phys. Rev. Lett. 85 (2000) 2240.
[10] M. Fukugita, C.J. Hogan and P.J.E. Peebles, Astrophys. J. 503 (1998) 518.
[11] C. Alcock *et al.*, Astrophys. J. 542 (2000) 281.
[12] T. Lasserre et al., Astronomy and Astrophys. 355 (2000) 39.
[13] K. Jedamzik, Phys. Rev. D 55 (1998) 5871.
[14] K.P. Rauch, Astrophys. J. 374 (1991) 83.
[15] R.B. Metcalf and J. Silk, Astrophys. J. 519 (1999) L1.
[16] M. Goliath and E. Mörtsell, Physics Letters B 486 (2000) 249.
[17] U. Seljak and D. Holz, Astronom. Astrophys. 351 (1999) L10.
[18] SNAP Science Proposal, available at `http://snap.lbl.gov` .
[19] J.F. Navarro, C.S. Frenk, and S.D.M. White, Astrophys. J. 490 (1997) 493.
[20] S. Ghigna, B. Moore, F. Governato, G. Lake, T. Quinn and J. Stadel, Astrophys. J. 544 (2000) 616.
[21] D.E. Holz, and R.M. Wald, Phys. Rev. D 58 (1998) 063501.

[22] L. Bergström, M. Goliath, A. Goobar, and E. Mörtsell, Astron. Astrophys. 358 (2000) 13.
[23] D. Huterer and M.S. Turner, Phys. Rev. D 60 (1999) 081301.
[24] M. Goliath, R. Amanullah, P. Astier, A. Goobar and R. Pain, *in preparation*.
[25] M. Tegmark, *pre-print* astro-ph/0101354 (2001).
[26] P. Schneider, J. Ehlers and E.E. Falco, *Gravitational Lenses* (Springer Verlag, Berlin, 1992).